00FCC-28

Development of a Sensor-less Speed Control Inverter for an Automotive Accessory Permanent Magnet Motor

Gui-Jia Su
Oak Ridge Institute for Science and Education

George W. Ott, and John W. McKeever
Oak Ridge National Laboratory

Kelly S. Samons, Roy L. Kessinger
Visual Computing System

Copyright © 1998 Society of Automotive Engineers, Inc.

ABSTRACT*

Visual Computing Systems (VCS) and Oak Ridge National Laboratory (ORNL) are partnered in a research effort to design and build a power inverter for use with an automotive accessory permanent magnet (PM) motor provided by VCS. The inverter is designed so it can fit within the volume of the housing, which is integrated with the motor. Moreover, a modular design for both the inverter and motor is employed for easily expanding the power capability to other applications. A simple back electromotive force (EMF) based position detection scheme is implemented with a digital signal processor (DSP) to eliminate the need for position sensors. Issues related to position detection errors are addressed and correction methods are suggested and implemented in DSP software. Finally, since the motor has very low inductance because of its coreless stator structure, the influences of the low inductance on the motor current ripple are analyzed. This analysis is used to design a fast current control loop for the inverter to cope with the low inductance. Analytical and experimental results are included to verify the proposed schemes.

INTRODUCTION

PM motors have higher efficiency due to the elimination of magnetizing current and copper loss in the rotor. It is also easier to achieve high performance torque control with PM motors, in particular brushless DC (BLDC) motors. Owing to these advantages, PM motors have already been widely used in a variety of applications in industrial automation and consumer electric appliances [1]. Recent advancements in PM materials have made PM motors a great candidate for traction motors in electrical vehicle applications.

VCS and ORNL are partnered in a research effort to design and build a power inverter for use with an automotive accessory PM motor provided by VCS. To reduce the cost and space requirement of the drive system, great attention is placed in the layout design of the inverter so that it can fit within the volume of the housing, which is integrated with the motor. Although the motor has a rated shaft power of 8 kW with a maximum speed of 4000 rpm, a modular design approach for both the inverter and motor is employed for easily expanding the power capability to other application needs.

There are mainly two ways to excite a PM motor. One is to drive the motor in synchronous AC mode in which a three-phase sinusoidal current is delivered to a motor that has a sinusoidal back EMF. The other excitation scheme, which has been proved particularly attractive for high power drive systems and is thus the choice for the accessory motor drive, is for BLDC motors. It consists of a three-phase PM motor with a trapezoidal back EMF excited by quasi-square current waveforms. This excitation can be conveniently accomplished with a three-phase full-bridge voltage source inverter. An attractive feature of this approach is the resulting simplicity of inverter phase sequencing. The flat top of the trapezoidal back EMF waveform is well matched to the quasi-square wave current waveform that can be produced by a voltage source inverter, lending itself to a

* Prepared by the Oak Ridge National Laboratory, Oak Ridge, Tennessee 37831, managed by Lockheed Martin Energy Research Corporation for the U.S. Department of Energy under contract DE-AC05-96OR22464.
The submitted manuscript has been authored by a contractor of the U.S. Government under Contract No. DE-AC05-96OR22464. Accordingly, the U.S. Government retains a non-exclusive, royalty-free license to publish from the contribution, or allow others to do so, for U.S. Government purposes.

low cost drive system (refer to Fig. 1). One disadvantage of the trapezoidal back EMF waveform is the requirement for accurate stator current commutation control. The torque developed in a PM motor with a trapezoidal back EMF is very sensitive to the relative phase of the quasi-square wave currents imposed by the inverter with respect to the back EMFs. A small phase error in commutation can produce significant pulsating torques in such drives. Accurate phase information of the back EMF is thus required to properly commutate the stator currents with an inverter.

While the required phase information has conventionally been provided by using position sensors, such as a shaft mounted encoder or built-in hall sensors [2][3][4][5], sensor-less control is desired to reduce cost and to improve reliability. Furthermore, it is the only choice for some applications where those sensors can not function reliably [1][6][7]. Advantages of position sensor based control include: 1) availability of position information even at very low speed resulting in a wider speed control range; and 2) better dynamic speed control performance. The disadvantages are: 1) added components and cost; and 2) lower reliability due to more signal wiring.

A simple back EMF based position detection scheme is implemented with a DSP to eliminate the need for position sensors. The DSP also controls motor speed and current. Issues related to position detection errors are addressed and methods of error correction are suggested and implemented in DSP software. Advantages of the position sensor-less control are: 1) reduced cost by elimination of position sensors; and 2) improved reliability by using fewer components and less signal wiring. The disadvantages are: 1) back EMF signals that are difficult to detect at very low speeds resulting in a narrow speed control range; and 2) lower dynamic speed control performance due to the limited resolution of speed detection. For applications such as the automotive accessory motors where the motors are not intended to run at very low speeds, the back EMF based sensor-less control is able to meet the performance requirements for speed regulation.

Due to their large effective air gaps, PM motors tend to have low inductance. The use of a coreless stator in the VCS motor has further reduced the inductance (<100μH). While these types of very low inductance PM motors have fast current control response and a linear relationship between current and its developed torque, they demand stringent current regulation for the inverter to obtain acceptable current ripple. The problem becomes even more serious with high-speed motors. Such motors will be increasingly used due to their compact size [7][8]. An analysis of the influence of the low inductance on current ripple has been used to design a fast current control loop thereby enabling the inverter to cope with low inductance. Analytical and experimental results are included to verify the proposed schemes.

SENSOR-LESS CONTROL

BRUSHLESS DC MOTOR

Fig. 1 shows the excitation for a BLDC motor that consists of a PM motor with a trapezoidal back EMF excited by a three-phase current source. The source can be provided by a current controlled voltage source inverter. The PM motor is represented by an equivalent circuit consisting of a stator resistance, inductance, and back EMF connected in series for each of the three phases with the mechanical moving portion omitted. The figure also shows the desired stator currents that the current source should provide and their relationship with the back EMFs. The currents in each phase have a rectangular wave-shape and must be in phase with the back EMFs of the corresponding phase. In this way, the flat top of the trapezoidal back EMF waveform is well matched to the quasi-square wave current waveform that can be produced by a voltage source inverter, lending itself to a low cost drive system. Such currents will develop a constant power and thus torque delivered to the rotor. To be able to provide such currents, we need to know the rotor position information related to the angular phase of the back EMFs. The phase information of the six points per electrical cycle marked by arrows in the figure is sufficient to control a BLDC motor.

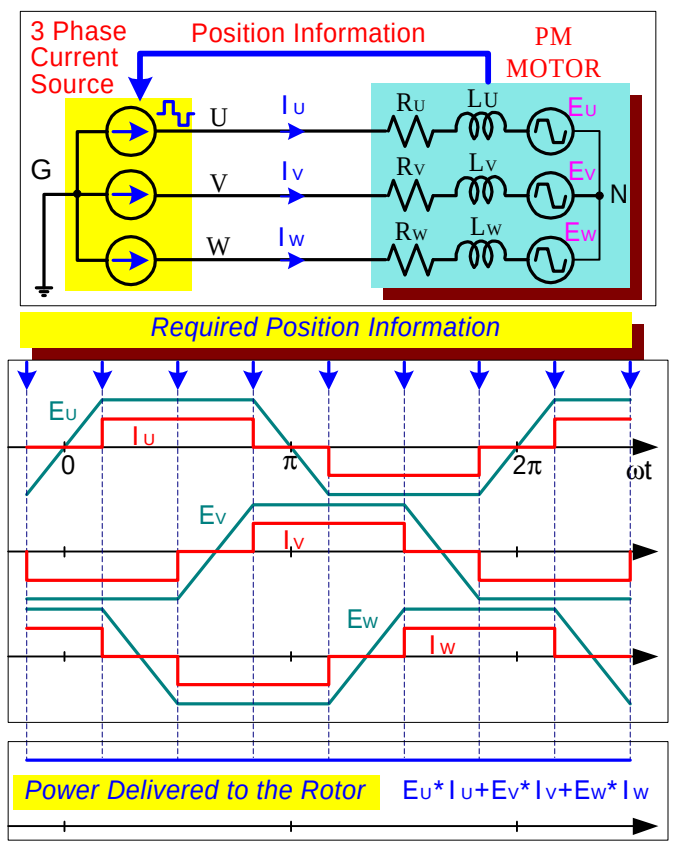

Fig. 1 Excitation of Brushless DC motors.

POSITION DETECTION BASED ON INDIRECT MEASUREMENT OF BACK EMF

Fig. 2 illustrates the principle of position detection based on indirectly measuring the back EMFs. E_{U1}, E_{V1} and E_{W1} are the fundamental components of the back EMFs, E_U, E_V and E_W, respectively. Comparing the relationship between these waveforms reveals that the phase positions needed for commutation control correspond to the peak points of the fundamental waveforms. So all one needs to do is to extract the fundamental components and detect their peak points. A functional block diagram of the suggested position detection is also shown in the figure. Because the back EMFs can be derived from the motor terminal voltages, motor terminal voltages are measured through a voltage divider of a resistor network and passed through a low-pass filter to obtain the fundamental components of back EMFs. Since zero-crossing detection is preferred to peak detection, an integrator is inserted to convert the peak points into zero-crossing points. The use of an integrator produces a signal of fixed amplitude that is dependent on the back EMF constant but independent of motor speed. Motor speed information can also be obtained by measuring the frequency of the detected signals.

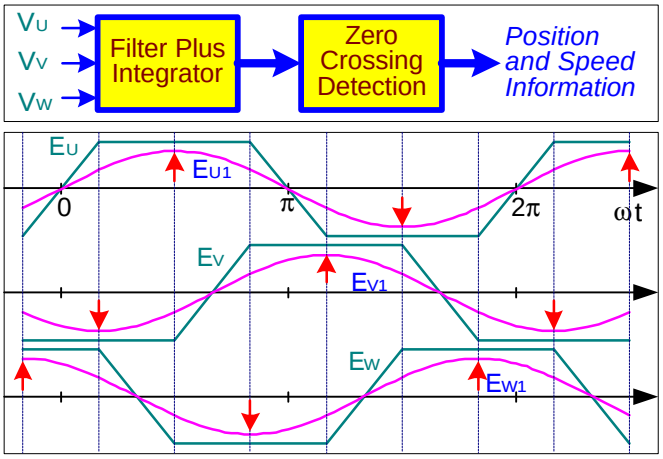

Fig. 2 Principle of position detection.

ERROR CORRECTION IN POSITION DETECTION

Since low-pass filters are employed to extract the fundamental components of back EMF waveforms, they will inevitably introduce phase shifts into the measured fundamental components and in turn produce errors in the detected position information. Further, the phase-shift varies with the back EMF frequency, i.e. motor speed. The graph shown in Fig. 3 plots phase errors versus back EMF frequency for a typical filter design. Obviously the phase shift is too big to be ignored at low motor speed. To satisfactorily operate a motor at low speed we have devised a software method to correct the phase errors.

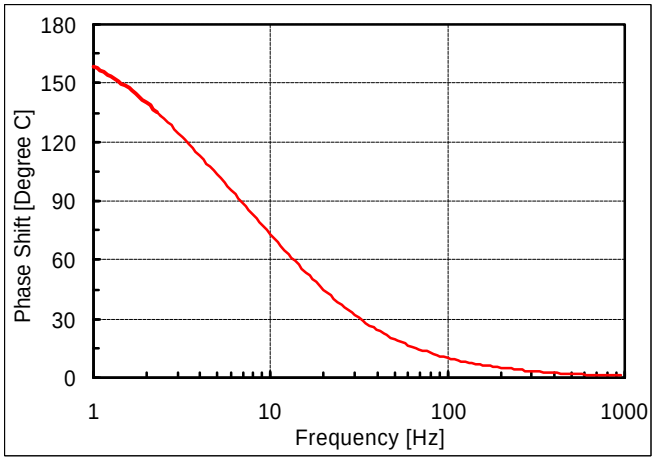

Fig. 3 Phase errors v.s. frequency for a typical filter design.

One disadvantage of the trapezoidal back EMF waveform is the need for accurate current commutation control. The developed torque in a PM motor with a trapezoidal back EMF is very sensitive to the relative phase of the quasi-square wave currents delivered by the inverter in response to the back EMF signals. A small phase error in commutation can produce significant pulsating torques in such drives. Fig. 4 gives an example where the currents are leading the back EMFs by 30 electrical degrees. For this condition the power and thus the torque delivered to the rotor is no longer constant but fluctuates to introduce a notch at every commutation.

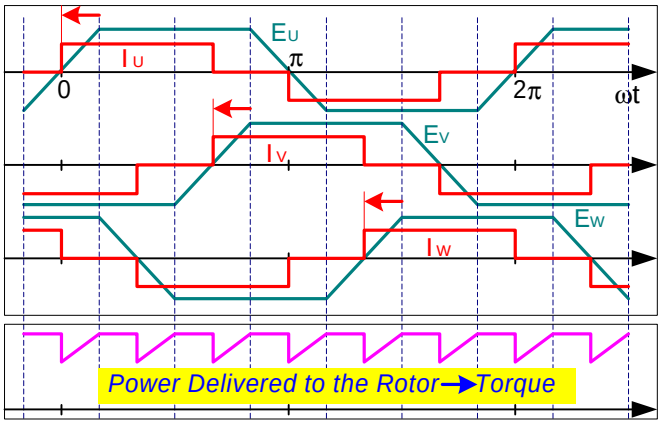

Fig.4 Torque ripples due to current leading back EMF.

Fig. 5 shows a modified block diagram of position detection where a phase error correction block is added. The correction is determined by a look-up table since, once the filter is designed, the resulting phase shift information can be calculated. Another source of error is the voltage drop across the stator impedance, which also becomes significant at low speed. This error can be eliminated by measuring the currents and the stator impedance.

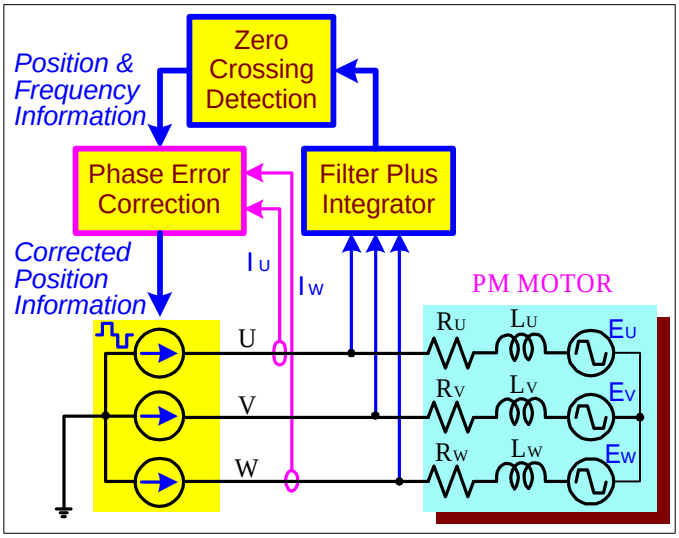

Fig. 5 Block diagram of modified position detection.

DSP BASED IMPLEMENTATION OF SENSOR-LESS CONTROL

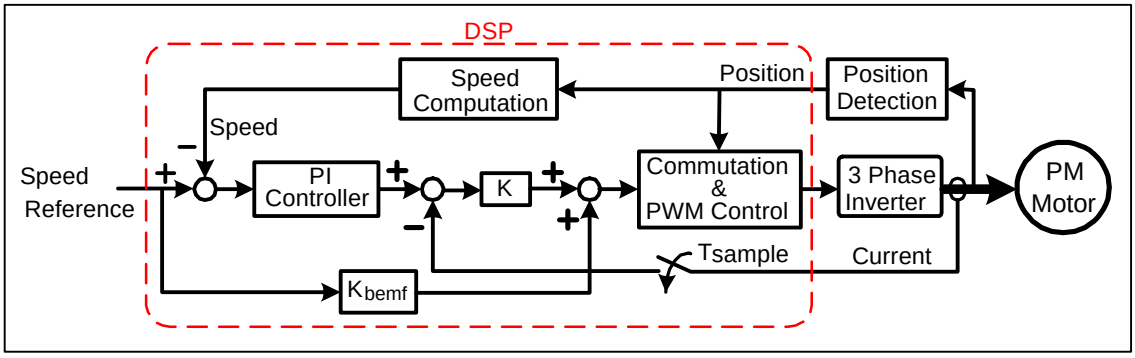

Fig. 7 Sensor-less speed control block diagram.

CURRENT RIPPLE ANALYSIS

The influences of the low inductance on the current ripple can be analyzed based on an equivalent circuit for a BLDC motor with trapezoidal back EMF driven by a standard bridge inverter, as shown in Fig. 8. Notice that phase commutation is not considered in the equivalent circuit. Ignoring the state coil resistance, R_m, the peak value of stator current ripple at steady state in the continuous conduction mode can be determined by the following equation.

$$I_{mripple(Peak)} = \frac{1}{4L_m f_{SW}}\left(1-\frac{K_{emf}N}{V_{dc}}\right)K_{emf}N$$

where

L_m is the phase leakage inductance, henries,
f_{SW} is the switching frequency, Hz,
V_{dc} is the inverter DC link voltage, volts,
K_{emf} is the back EMF constant, volts/RPM, and
N is the motor speed, RPM.

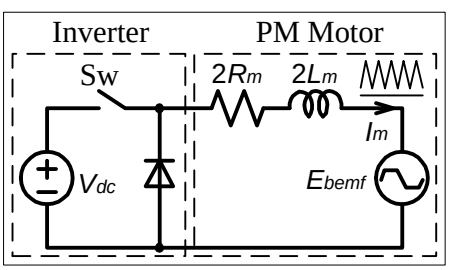

Fig. 8 An equivalent circuit for BLDC motor drive.

A plot of current ripple versus speed is given in Fig. 9 for the accessory motor at f_{SW}=20kHz, V_{dc}=320V. The motor has a rated shaft power of 8 kW and a measured phase inductance, L_m, of 65μH. As indicated in the graph, the current ripple is quite high over the speed range of 1000 rpm to 3500 rpm even at a switching frequency of 20 kHz, which is about the limit for IGBTs. This shows how challenging it is to regulate the current ripple for this type of low inductance motor. It is also interesting to notice that the maximum current ripple occurs at the speed where the back EMF is equal to half the DC bus voltage, which is around the middle of the operating speed rage.

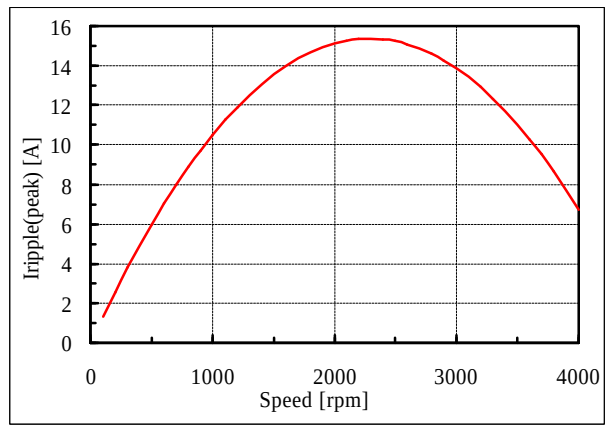

Fig. 9 Current ripple v.s. motor speed.

SIMULATION AND EXPERIMENTAL RESULTS

Fig. 10 shows a comparison of typical motor currents and the developed torque waveforms between a case where the currents are leading the corresponding phase back EMFs by 30 electrical degrees [Fig. 10(a)] and a case where the currents are in phase with the back EMFs [Fig. 10(b)]. These are generated by digital computer simulations, where the inverter switches at 20 kHz and the fundamental frequency of current is set for 250 Hz.

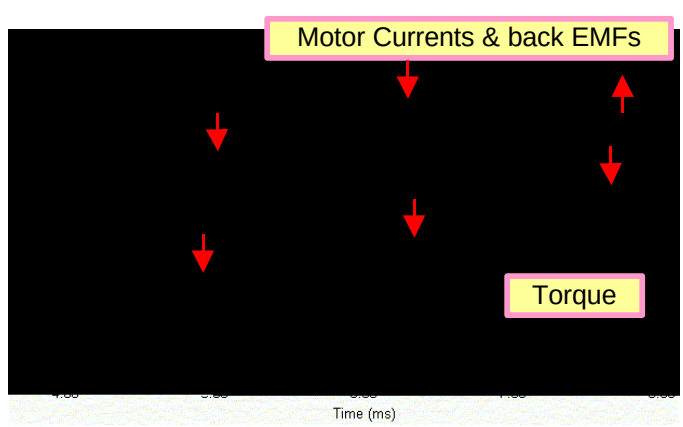

(a) Motor currents are leading the phase back EMFs by 30 degrees.

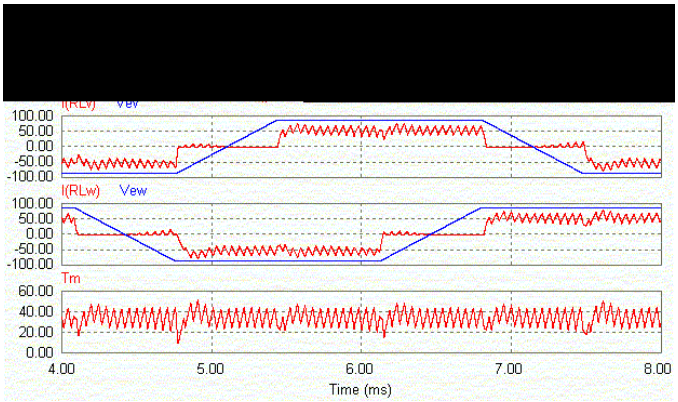

(b) Motor currents are in phase with the back EMFs.

Fig. 10 Comparison of motor currents and torque waveforms.

The differences between the two cases are that current bumps, marked by arrows, occur at the beginning of each half cycle when the currents are out of phase with the back EMFs. The current bumps result from the shorting of the corresponding two phase back EMFs through the conducting IGBT of the lower devices and the diode associated with the lower IGBT of the open leg. Take phase U for instance and refer to Figs. 4 and 6. At the beginning of each negative half cycle when the current is commutated from S_6 to S_4 while S_2 is conducting, the diode of S_6 is positively biased over the first period of 30 degrees during which back EMF, E_U, is greater than E_W. Therefore, the two phase back EMFs are shorted through the diode and S_4, and consequently a current bump is produced. Similarly at the beginning of each positive half cycle when the current is commutated from S_4 to S_5 while S_3 is conducting, the two phase back EMFs E_V and E_U are shorted through S_5 and the diode associated with S_4. The deteriorated current waveforms also produce large torque pulsations as is evident from the sizeable differences in the torque waveforms shown in Fig. 10(a).

Every time the stator current is commutated from one phase to another, a torque pulsation is also generated even when the phase currents are properly switched from one to another as can been seen in Fig. 10(b). Again the magnitude of the pulsation depends on the inductance and operating current, and a low inductance helps to reduce the magnitude. In addition to these pulsations, high frequency torque pulsations also occur due to the current ripples produced by the PWM

CONTACT

sugj@ornl.gov
http://www.ornl.gov/etd/peemrc

REFERENCES

1. D. M. Erdman, H. B. Harms, J. L. Oldenkamp, "Electronically Commutated DC Motors for the Appliance Industry," *Conf. Rec. 1984 IEEE Ind. Applicat. Soc. Ann. Mtg.*, pp. 1339-1345.
2. M. Lajoie-Mazenc, C. Villanueva, J. Hector, "Study and Implementation of Hysteresis Controlled Inverter on a Permanent Magnet Synchronous Machine," *Conf. Rec. 1984 IEEE Ind. Applicat. Soc. Ann. Mtg.*, pp. 426-430.
3. C. Bergmann, P. Goreau. J. P. Louis, "Direct Digital Control of a Self-Controlled Synchronous Motor with Permanent Magnet," 1st European Conf. on Power Electronics and Applications, pp. 3.269-3.273, October 1985.
4. A. Kusko, S. M. Peeran, "Brushless DC Motors Using Unsymmetrical Field Magnetization," *Conf. Rec. 1986 IEEE Ind. Applicat. Soc. Ann. Mtg.*, pp. 774-780.
5. B. V. Murty, "Fast Response Reversible Brushless DC Drive with Regenerative Breaking," *Conf. Rec. 1984 IEEE Ind. Applicat. Soc. Ann. Mtg.*, pp. 445-450.
6. T. Endo, F. Tajima, H. Okuda, K. Iizuka, Y. Kawaguchi, H. Uzuhashi, Y. Okada, "Microcomputer-Controlled Brushless Motor without a Shaft-Mounted Position Sensor," *IPEC-Tokyo'83 Conf. Record*, pp. 1477-1488, March 1983.
7. I. Takahashi, T. Koganezawa, G. J. Su, K. Ohyama, "A Super High Speed PM Motor Drive System by a Quasi-Current Source Inverter", *IEEE trans. Ind. Applicat.*, Vol. 30, pp. 683-690, May/June 1994.
8. F. Caricchi, F. Crescimbini, O. Honorati, G. Lo Bianco, E. Santini, "Performance of Coreless-Winding Axial-Flux Permanent-Magnet Generator with Power Output at 400 Hz, 3000 r/min", *IEEE trans. Ind. Applicat.*, Vol. 34, pp. 1263-1269, Nov./Dec. 1998.
9. "TMS320C24x DSP Controllers Reference Set," Texas Instruments, 1997.